



Evolution of Alkali Release by an Illitic Rock for Use as Supplementary Cementitious Material

Roxana Lemma · Silvina Marfil ·
Viviana Rahhal

Accepted: 4 October 2022 / Published online: 20 October 2022
© The Author(s), under exclusive licence to The Clay Minerals Society 2022

Abstract The levels of CO₂ emissions generated by the cement industry and the growth in demand for its products have led to a search for ways to reduce these emissions. The use of supplementary cementitious materials has become one of the solutions proposed for this problem. Illite, which is found all over the world, is a possible supplementary cementitious material. Before illite can be used, it must be milled and treated thermally in order to activate it, so that the alkalis (Na⁺ and K⁺) are free and available to react. Alkalis in cement participate in deleterious reactions (alkali-silica reaction) or have a beneficial effect (alkaline activation). The alkalis present in the rocks can play an active role in these phenomena, however. In addition, the material could be influenced by the alkaline environment produced by the cement. The current study was aimed at analyzing whether an alkali release occurs and if so, how it is affected when a milled and thermally treated illitic rock is in contact with water or an alkaline solution. The material was characterized by X-ray fluorescence, polarizing microscopy, and X-ray diffraction

(XRD). The sample was treated thermally at 300, 600, and 900°C, and the thermal activation was evaluated through XRD, density, and Atterberg limits. The evolution of alkali release was studied by determining the sodium and potassium concentration of contact water obtained by mixing the samples with different pH solutions for various lengths of time. In addition, the calcium concentration was determined. The concentrations of sodium and potassium in the contact water were determined by flame photometry, and of calcium by EDTA (ethylenediaminetetraacetic acid) titration. The results showed that with increasing age, increasing solution pH, and higher treatment temperatures, alkali release occurred and increased, whereas Ca²⁺ concentration decreased.

Keywords Alkalis · Cement · Clay · Emissions · Greenhouse gas · Illite · Supplementary cementitious material

Introduction

Concern about the environment has increased in recent years across all types of industry. The cement industry, over the past 65 years, has seen its production increase almost 34-fold; its emissions represent 5–8% of all anthropogenic greenhouse gases (Mikulčić et al., 2016; Scrivener et al., 2018; Tam et al., 2009). The industry, other organizations, and researchers have sought ways to reduce these CO₂

Associate Editor: Chun Hui Zhou

R. Lemma (✉) · V. Rahhal
Facultad de Ingeniería, CIFICEN (UNCPBA-CONICET-CICPBA) – Olavarría, Buenos Aires, Argentina
e-mail: roxana.lemma@fio.unicen.edu.ar

S. Marfil
Dpto. de Geología, Universidad Nacional del Sur.
CGAMA-CIC., Bahía Blanca, Buenos Aires, Argentina

emissions. The use of supplementary cementitious materials (SCM) is generally agreed as a good way forward (Mikulčić et al., 2016; Scrivener et al., 2018); in particular, calcined clays are favored, because of their wide availability, favorable behavior, and lower energy consumption (ACI Committee 232, 2012; Benhelal et al., 2021).

Thermally treated kaolin (metakaolin) is the most studied calcined clay to be used as a SCM, and numerous authors have shown that it is suitable for this purpose because of its good strength and durable behavior (Almenares et al., 2017; Fernandez et al., 2011; Sabir et al., 2001; Trümer & Ludwig, 2015). Illite has also been used and is readily available in various parts of the world (Nickovic et al., 2012), especially in the Argentine cement production zone (Zalba et al., 2010). In Argentina, the first study of thermally treated illite from the province of Buenos Aires to be used as a SCM dates back to 1971 (Batic et al., 1971), but it did not provide satisfactory strength results because of a low treatment temperature. Although at the correct activation temperature, $\sim 900^\circ\text{C}$ (He et al., 1995a; Jiang et al., 2008; Lemma et al., 2015), illite has a lower reactivity than metakaolin, many studies show that thermally treated illite also performs well (ACI Committee 232, 2012; Ambroise et al., 1985; Cordoba et al., 2020; Cordoba & Irassar, 2021; He et al., 1995a; He et al., 1995b; Irassar et al., 2019; Lemma et al., 2015, 2018; Marchetti et al., 2020; Trümer & Ludwig, 2015). He et al. (1995a) reported that with a 30% replacement of portland cement by illite treated at 930°C , a mortar compressive strength greater than that of the inert mortar (quartz replacement) was obtained after 7 days of aging, but it never reached that of the ordinary portland cement (OPC) reference mortar. Marchetti et al. (2020) found that mortars with 25% replacement by illite treated at 950°C for OPC reached the same compressive strength as the OPC mortar after 90 days. Cordoba et al. (2020) and Cordoba and Irassar (2021) found that in a sorptivity test, at 28 days, the initial rate of water absorption was the same for a portland cement concrete and a concrete containing 25% calcined illite in place of OPC. Furthermore, in mortars with 20% calcined illite, the expansion due to sulfate attack was controlled in a cement with a large C_3A content.

However, cement has alkalis (Na and K) in its chemical composition. For many years, expansion

due to the alkali-silica reaction (ASR) was believed to be unlikely when the alkali content of the portland cement was $<0.6\% \text{Na}_2\text{O}_{\text{eq}}$. This consideration was adopted in the ASTM C150 standard. The ASR occurs when the alkalis from the paste react with the amorphous silica of aggregates, forming an expansive gel around them, which produces concrete cracking. Nevertheless, it is now recognized that limiting the alkali content in cement is not an effective way of preventing the ASR because it does not control the total alkali content of the concrete mixture. Therefore, limiting the expansion is an effective way of controlling the ASR (Folliard et al., 2003).

The alkali content of the concrete mixture could be affected by the alkalis provided mainly by the portland cement, SCM, aggregates, and additives. Some thermally treated clays used as SCM also have alkalis in their chemical composition (Grim, 1942). Furthermore, illite has potassium in its structure as an interlayer cation (Bailey, 1984). When it is extracted from the soil to be used as SCM, it is in the form of illite-rich rocks which also have other mineral components such as quartz, feldspars, chlorite, and iron oxides. Some of these minerals also have alkalis in their compositions, so alkalis could be provided by them. Rossetti et al. (2018) studied the ASR expansion of mortars with a 20% replacement by calcined illite. Portland cement with high and low alkali content was used, and the results showed that when the high-alkali-content cement was used, the expansion of the mortars with the calcined illite replacement was less than that of the OPC mortar. When the low-alkali-content cement was used, the expansion of the mortars with the calcined illite replacement was greater than in the OPC mortar.

On the other hand, alkalis could be used to stimulate the reactions and to make geopolymer binders. Experience has shown that calcined clays have potential in this area (Buchwald et al., 2009; Diop & Grutzeck, 2008; Hu et al., 2017; Marsh et al., 2018; Werling et al., 2022). Buchwald et al. (2009) found that common clays such as illite-smectite are suitable as raw materials for preparing geopolymer binders. They studied the dissolution of silicate and aluminate monomers from clays in an alkaline solution and concluded that the best performance as geopolymer binders can be attained by thermal treatment of the clay minerals. However, the highest rate of dissolution was reached by metakaolin.

When illite is treated thermally to be used as a SCM, the dehydroxylation process must occur to make it reactive (He et al., 1995a). Dehydroxylation consists of the loss of the OH^- groups due to high temperature, which results in the destruction of the structure, making the aluminosilicates amorphous and reactive (Buchwald et al., 2009). In addition, some of the secondary minerals present in the rock could go through dehydroxylation at lower temperatures than illite. In this case, therefore, alkalis could be free to participate in the reactions. Furthermore, when illite and secondary minerals are in contact with the cement pore solution, in a high-pH alkaline environment, (Behnood et al., 2016), the properties of the clay minerals (Abedi Koupai et al., 2020; Carroll & Starkey, 1971; Sruthi & Reddy, 2020) and the release of their alkalis could be affected.

The present study aimed, therefore, to analyze alkali release from an illitic rock at various treatment temperatures in various pH systems.

The hypothesis tested was that alkali release occurs when the thermally treated illitic rock is milled and mixed with water or an alkaline solution; and also that it will be modified by the treatment temperature of the sample and the pH of the contact solution.

Materials and Methods

The material tested was an illitic rock from a quarry located in the province of Buenos Aires (Argentina) near the city of Olavarría (Fig. 1), which corresponds to the Sierras Bayas Group, Cerro Negro Formation (Neoproterozoic) in the Sierras Septentrionales of the Province of Buenos Aires. The Sierras Septentrionales have the oldest rocks in Argentina. Igneous and metamorphic rocks constitute the basement, known as the Buenos Aires Complex (Paleoproterozoic). The Complex is covered partially by three sedimentary units, the Sierras Bayas Group (Neoproterozoic) and the Cerro Negro and Balcarce Formations (Eopaleozoic), formed in a shallow sea. The Sierras Bayas Group is 167 m thick and comprises four depositional successions separated by regional unconformities. From the base to the top, it is composed of quartzarkosic sandstones, dolomites, and shale, followed by quartz sandstones, claystones, and dark micritic limestones. The Cerro Negro Formation consists of >100 m of claystone with heterolithic intercalations. The Balcarce Formation, 100 m thick, represents a sequence of quartz sandstones with subordinate claystones and fine-grained conglomerates (Dalla Salda et al., 2006).

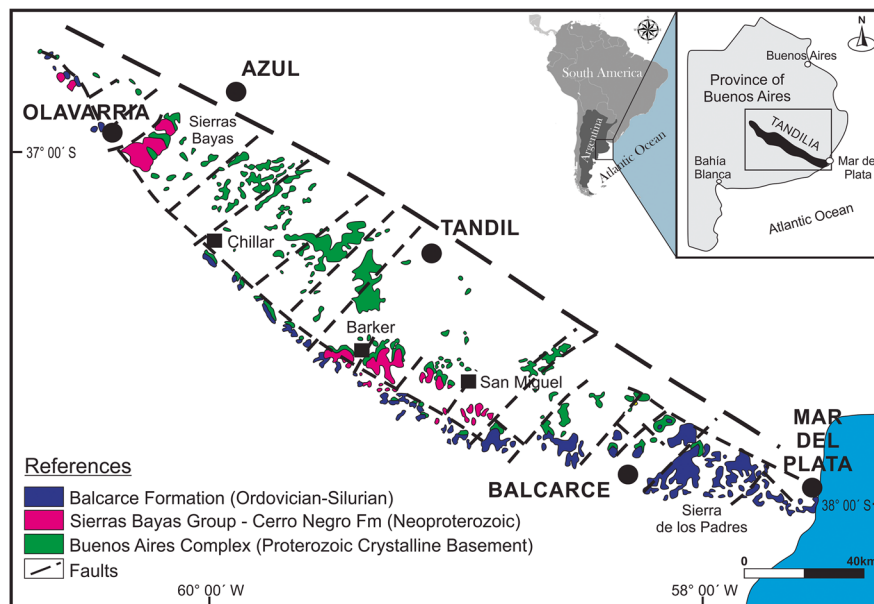


Fig. 1 Geological sketch of the Sierras Septentrionales of the Province of Buenos Aires and location of the study area (Olavarría) (modified from Cingolani (2011) and Pérez Marfil et al. (2021))

The Cerro Negro Formation (Sierras Bayas Group) (Fig. 1) is a sedimentary unit with few outcrops. The basal section, in the Olavarría area, has up to 12 m of marl and reddish flakes that rest on the limestone of the Loma Negra Formation (Barrio et al., 1991). Those authors described three associations of sedimentary facies that, from base to top, are: (1) slope breccia, chert, and mudstones; (2) mudstones with planar stratification and mudstones; and (3) mudstones with wave stratification. A clearly pelitic member of illite-chlorite composition has developed.

After extraction, the rock was milled until <12% was retained in the #325 sieve and homogenized. Chemical analysis of the whole rock was done by X-ray fluorescence (XRF), using a Malvern Panalytical Axios Fast instrument (Malvern Panalytical, Almelo, The Netherlands). The mineralogical composition was determined by polarizing microscopy and XRD. A Leica DM750 P (Leica Microsystems, Wetzlar, Germany) microscope was used for the petrographic study of thin sections and a Philips X'Pert PW 3710 (Philips, Eindhoven, The Netherlands) X-ray diffractometer with $\text{CuK}\alpha$ radiation and a graphite monochromator, working at 40 kV and 20 mA, for XRD.

In order to improve the identification of clay minerals by XRD, the clay fraction was separated by decantation in a cylinder burette for 2 h. A portion of the suspension was removed and spread on a slide. The clay fraction was analyzed using a Rigaku D-Max III-C diffractometer (Rigaku, Tokyo, Japan), working at 35 kV and 15 mA, using $\text{CuK}\alpha_{1,2}$ radiation ($\lambda = 1.541840 \text{ \AA}$) filtered with a graphite monochromator in the diffracted beam, from 3 to $40^\circ 2\theta$ with increments of $0.02^\circ 2\theta$ and a counting time of 2 s per step.

For all the determinations, the sample consisted of the whole milled rock. The sample was activated thermally at 900°C , which is the dehydroxylation temperature of illite (He et al., 1995a; Jiang et al., 2008; Lemma et al., 2015), to achieve the best performance as SCM. The sample was also treated at intermediate temperatures (300 and 600°C) to study its evolution behavior with temperature increase. The thermal treatment was carried out in a muffle furnace for 90 min at constant temperature. The density was determined using the Le Chatelier volumometer,

and the Atterberg limits were determined according to ASTM D4318-17.

The evolution of alkali release was studied by determining the sodium and potassium concentrations of contact water obtained from samples mixed with various solutions (liquid/solid ratio of 10:1). The calcium concentration was also determined. Three solutions were used: a neutral one (initial pH ~ 7) with distilled water (N solution), and two alkaline solutions (initial pH ~ 13), one with 135 mmol/L $\text{Ca}(\text{OH})_2$ in distilled water (Ca solution) and the other with 135 mmol/L $\text{Ca}(\text{OH})_2$, and 5 mmol/L NaOH in distilled water (Ca-Na solution), simulating the pH of concrete (Behnood et al., 2016). In total, twelve combinations obtained by mixing the raw clay with the three solutions at the three heating temperatures were studied (Table 1).

After mixing, the hydrated samples were kept in a stove at 40°C until they reached the test ages: 1 and 6 h and 7, 28, 60, and 90 days for samples in N and Ca solutions, and 7, 28, and 60 days for samples in Ca-Na solution. The contact-water concentrations were determined using a flame photometer (Zeltec ZF240, Dicrom Ingeniería S.A., Buenos Aires, Argentina) for sodium and potassium, and EDTA titration for calcium (at 40°C). The results were the averages of three determinations, and the standard deviations were $< \pm 5\%$.

Table 1 Names of combinations studied, calcination temperatures of the samples, and the types of solutions used

Name	Calcination temperature ($^\circ\text{C}$)	Initial solution pH
0-N	Raw clay	~ 7 (N solution)
300-N	300	
600-N	600	
900-N	900	
0-Ca	Raw clay	~ 13 (Ca solution)
300-Ca	300	
600-Ca	600	
900-Ca	900	
0-Ca-Na	Raw clay	~ 13 (Ca-Na solution)
300-Ca-Na	300	
600-Ca-Na	600	
900-Ca-Na	900	

Results

Material Characterization

The chemical analysis of the whole rock (Table 2) indicated the predominance of SiO_2 and Al_2O_3 , followed by Fe_2O_3 and a significant amount of alkalis (Na_2O and K_2O), especially potassium, the illitic interlayer cation (Grim, 1942).

The rock used in the study was a very fine-grained sedimentary rock classified as an illite siltstone, of yellowish-brown color and homogeneous grain size. It presented a microcrystalline granular texture under a polarizing microscope in thin section (Fig. 2). It was composed of equidimensional irregular grains of quartz with subordinate illite and iron oxides. Illite occurred as fine elongated crystals within quartz. The matrix consisted of very fine quartz, illite, and chlorite grains.

In the XRD pattern of the bulk sample (Fig. 3), reflections corresponding to quartz, feldspars, illite, chlorite, and magnetite were identified. The XRD

pattern of the clay fraction (Fig. 4) also showed reflections of quartz, illite, and chlorite, confirming that which was already observed in the polarizing microscope, the presence of illite and chlorite in the sample. The XRD pattern of the clay fraction showed a background increment due to the glass slide.

Finally, the rock had ~45% illite, according to previous studies (Irassar et al., 2019; Lemma et al., 2015) for which samples were taken in the same area and from the same formations.

Thermal Treatment

The XRD patterns of the raw and the thermally treated samples (Fig. 3) showed a decrease in the characteristic illite peaks as the treatment temperature increased. At 900°C, the main peaks appeared with low intensity because the dehydroxylation temperature of illite is ~900–950°C (He et al., 1995a; Jiang et al., 2008; Lemma et al., 2015), turning the clay into a meta-illite, so a small amount of illite was not entirely activated thermally. As in the illite peaks, the

Table 2 Chemical composition (mean and coefficient of variation from four measurements) of the raw sample

Oxide (wt.%)								
SiO_2	Al_2O_3	Fe_2O_3	CaO	MgO	Na_2O	K_2O	TiO_2	LOI
61.98	16.80	6.47	0.96	2.25	1.72	3.81	0.87	4.33
±0.08	±0.04	±0.01	±0.05	±0.01	±0.01	±0.00	±0.01	±0.07

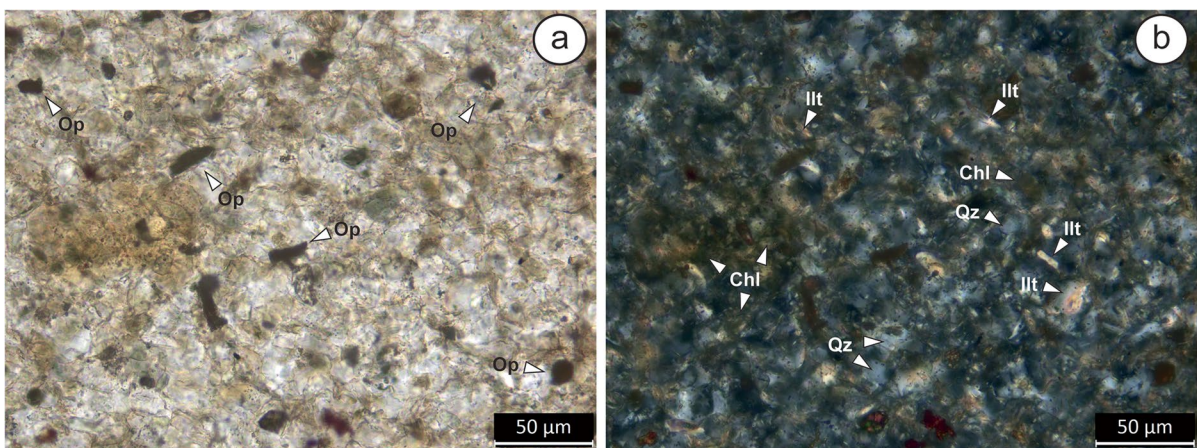


Fig. 2 Polarizing microscopy of thin sections. Mineralogical composition, structure, and texture of the rock **a** under parallel nicols, **b** under crossed nicols. Opaque minerals (Op), illite (Ill), chlorite (Chl), and quartz (Qz)

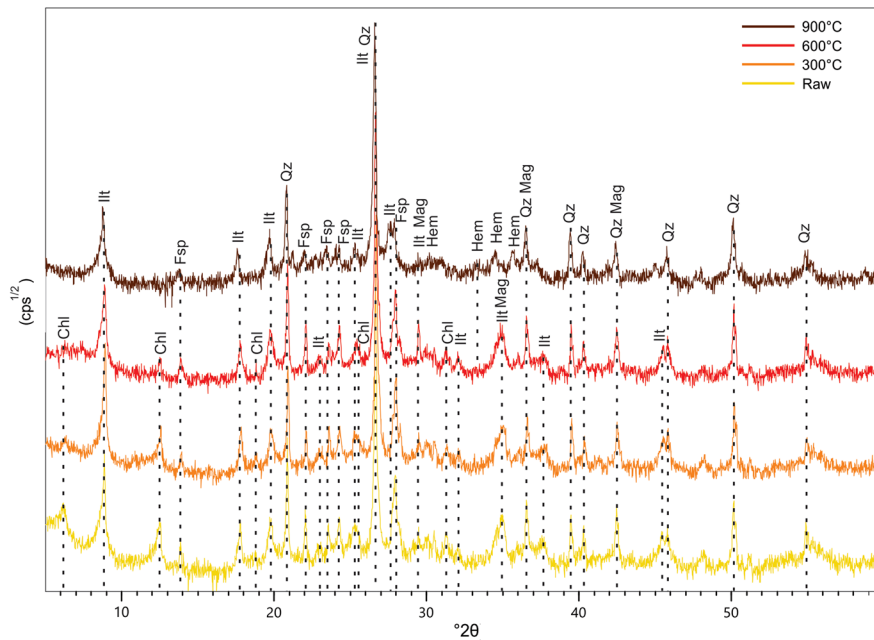


Fig. 3 XRD patterns for the raw sample and for samples treated at 300°C, 600°C, and 900°C. Chl: Chlorite, Ill: Illite, Fsp: Feldspar, Qz: Quartz, Mag: Magnetite, and Hem: Hematite

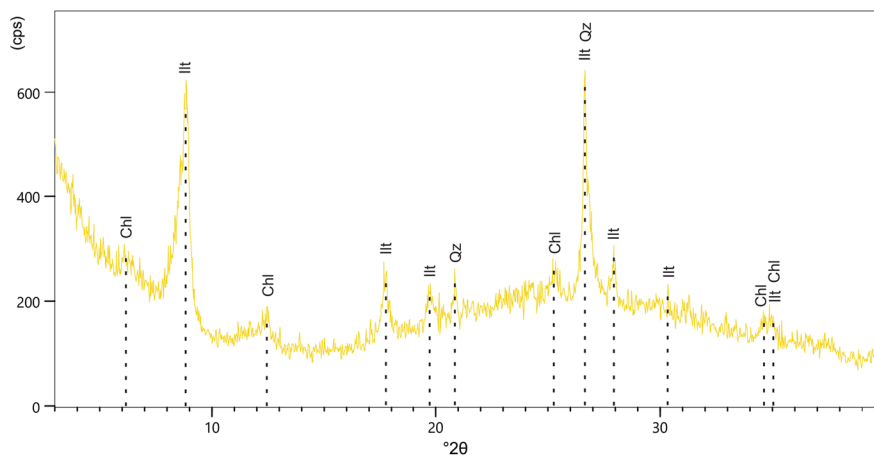


Fig. 4 XRD pattern of the clay fraction of the raw sample. Chl: Chlorite, Ill: Illite, and Qz: Quartz

chlorite peak intensities decreased with the treatment temperature increase, but in this case, the peaks disappeared after 600°C, showing a complete dehydroxylation of chlorite (Brindley & Ali, 1950). Quartz and feldspar peaks did not vary during the temperature increase. At 900°C, hematite peaks, responsible for the reddish color, appeared because of the change of Fe^{2+} to Fe^{3+} due to iron oxidation from magnetite

(Hanein et al., 2022; Murad & Wagner, 1996). Also observed was an increase in the background between 20 and 35° 2θ , which was related to the incremental increase in the amount of amorphous phase (He et al., 1995a).

The density and Atterberg limit results (Fig. 5) showed that the density increased with treatment temperature, but reached a maximum at 600°C.

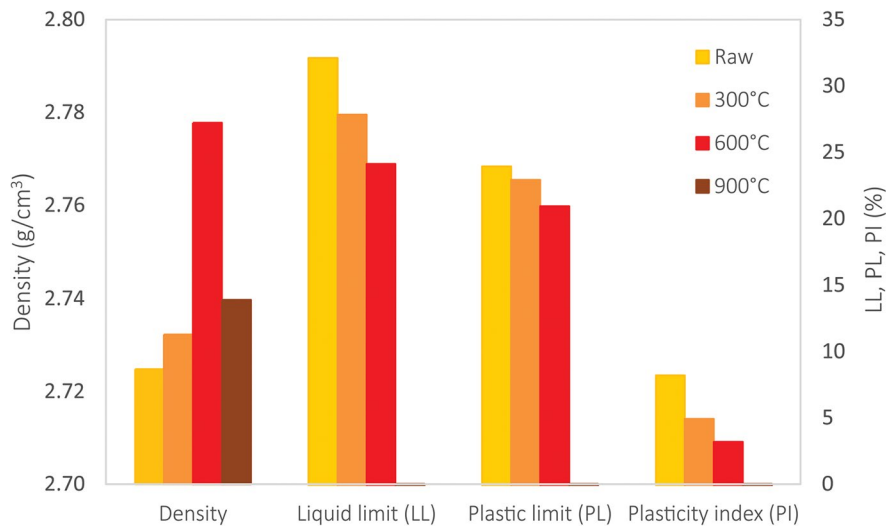


Fig. 5 Density, liquid limit (LL), plastic limit (PL), and plasticity index (PI) for raw and thermally treated samples

Moreover, the plasticity index decreased with increases in the treatment temperature until 600°C; at 900°C, the sample became non-plastic. The plasticity of a clay is due to its capacity to incorporate water (Andrade et al., 2011), so when the sample was treated thermally, the plasticity index reduction and the density increase could be related. At 900°C, some illite peaks in the XRD patterns (Fig. 3) disappeared as a consequence of dehydroxylation, which could result in structure collapse, thus accounting for a density decrease and the complete loss of plasticity. Batic et al. (1971) and He et al. (1995a) reported similar experiences. The former authors treated an illite at 600, 700, and 800°C, and the density increased and then decreased. In the same way, He et al. (1995a) treated another illite at 650, 790, and 930°C. The density increased in the samples with no thermal treatment and for those treated at 650°C, and then decreased for those treated at 790 and 930°C. This density decrease corresponded to the temperatures at which strength results were better.

Alkali Release and Calcium Concentration

Sodium ion concentration values in the contact water of samples (Fig. 6) showed an important difference in behavior among the samples in the different pH solutions. Samples in N solution had almost no variation with age, and their Na⁺ concentration was <1.5 mmol/L, whereas the samples in Ca and

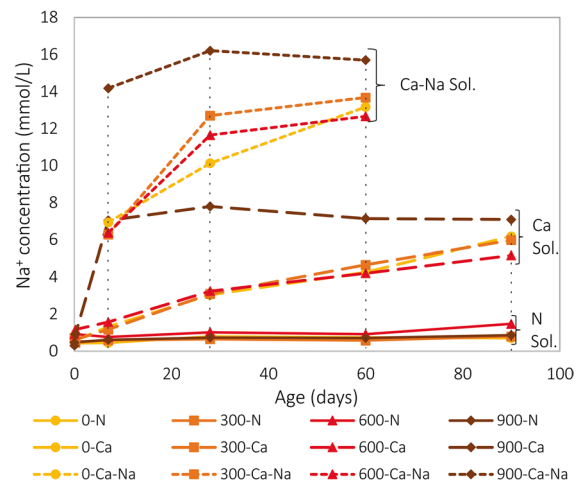


Fig. 6 Na⁺ concentration of contact water of raw and thermally treated samples in various pH solutions

Ca-Na solutions increased their Na⁺ concentration with age. For Ca solution, the raw sample and samples treated at 300 and 600°C had a similar behavior, reaching 5–7 mmol/L of Na⁺ at 90 days, but the sample treated at 900°C had a significant initial value at 7 days (~7.5 mmol/L of Na⁺) and then stabilized. For Ca-Na solution, in the raw sample and in those treated at 300 and 600°C, the Na⁺ concentration was similar at 7 days (6–7 mmol/L of Na⁺) and at 60 days (13–14 mmol/L of Na⁺), whereas the sample treated at 900°C had a greater initial value (14.18 mmol/L of

Na⁺ at 7 days) with an increase of ~2 mmol/L of Na⁺ at 28 days and then stabilized.

According to the percentage of Na₂O in the whole rock (1.72%), the theoretical maximum amount of Na⁺ available was 49.94 mmol/L, but samples in N solution released only 0.57–0.96 mmol/L of Na⁺ at 60 days. On the other hand, the addition of calcium to the solution (Ca solution) increased the Na⁺ concentration in the contact water of samples to 4.2–7.14 mmol/L at 60 days. Moreover, with the addition of calcium and sodium to the solution (Ca-Na solution) these values reached 12.66–15.7 mmol/L of Na⁺ at 60 days, considering that the Na⁺ concentration values of samples in Ca-Na solution had 5 mmol/L of NaOH provided by the solution.

Like the Na⁺ concentration, the K⁺ concentration in the contact water of samples increased with age (Fig. 7). According to the percentage of K₂O in the whole rock (3.81%), the theoretical maximum amount of K⁺ available was 72.96 mmol/L. However, samples in N solution exhibited a slight variation in K⁺ concentration with age, which remained at <0.1 mmol/L of K⁺. Samples in Ca solution showed similar behavior with respect to Na⁺ concentration, reaching ~0.4 mmol/L of K⁺ at 90 days in the raw sample and that treated at 300°C, and 1.2 mmol/L of K⁺ at 90 days in the sample treated at 900°C. However, the sample treated at 600°C showed an intermediate behavior in K⁺ concentration between samples treated at 300 and 900°C. For

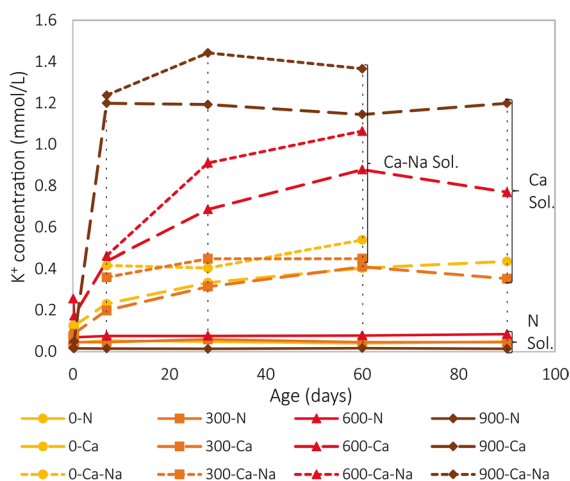


Fig. 7 K⁺ concentration of contact water of raw and thermally treated samples in various pH solutions

Ca-Na solution, the raw sample and that treated at 300°C had similar values to those for Ca solution. But samples treated at 600 and 900°C reached 1.06 and 1.37 mmol/L of K⁺ at 60 days, respectively.

While sodium and potassium concentrations increased with age, calcium concentration (Fig. 8), in general, decreased. Ca²⁺ concentration in the contact water for samples in N solution remained <1 mmol/L, even though the theoretical maximum amount of available Ca²⁺ in the whole rock was 15.43 mmol/L (0.96% CaO). With the addition of Ca(OH)₂, this value reached 15.57 mmol/L of Ca²⁺. However, the initial concentration in the contact water was ~14 mmol/L of Ca²⁺ for samples in Ca and Ca-Na solutions, which was similar to that of a Ca(OH)₂ saturated solution at 40°C.

The Ca²⁺ concentration in the contact water of samples in Ca and Ca-Na solutions exhibited similar behavior. Raw samples and those treated at 300°C showed a slight concentration decrease with age. Then, in samples treated at 600°C the decrease in Ca²⁺ concentration was more significant. Moreover, samples treated at 900°C showed a sharp decrease in the Ca²⁺ concentration at early ages; and after 28 days, the values were <1 mmol/L of Ca²⁺.

The effect of adding NaOH to the Ca-Na solution was the displacement of the results to slightly lower values. This effect was most evident at 7 days. After that, values tended to

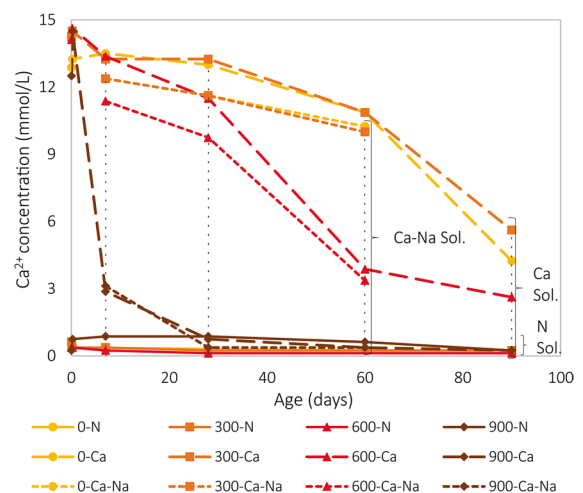


Fig. 8 Ca²⁺ concentration of contact water of raw and thermally treated samples in various pH solutions

approach those of the Ca solution. This effect was not visible for samples treated at 900°C because insufficient Ca was available.

Discussion

Comparison between the concentrations of Na^+ and K^+ in samples in the various solutions showed an important influence of the pH solution on alkali release. $\text{Ca}(\text{OH})_2$ incorporation into the solution increased the release of the Na^+ and K^+ in samples, and adding NaOH increased it further.

Rossetti et al. (2018) reported a similar experience with the pore solution of pastes made with a low-alkali portland cement, a 25% replacement of two illitic clays calcined at 950°C and water. When the calcined illite had a small alkali content (0.08% Na_2O and 5.60% K_2O), the pore solution decreased the Na^+ and K^+ concentration between 7 and 14 days of age, which Rossetti et al. (2018) attributed to their combination with silica and amorphous alumina in a pozzolanic reaction (ACI Committee 232, 2012). However, when the calcined illite had a large alkali content (1.52% Na_2O and 4.29% K_2O), the pore solution increased the Na^+ and K^+ concentration when similarly aged, the alkali release being greater than when combined in the pozzolanic reaction. The latter highlights the importance of Na content in alkali release, as occurred during the current investigation.

Furthermore, samples in Ca and Ca-Na solutions showed an increase in alkali release with increases in treatment temperature, which could be related to the modification of the clay structure. In previous publications (Lemma et al., 2015), stimulation of the reactions was seen through the strength improvement with increases in the treatment temperature.

On the other hand, the Ca^{2+} concentration of samples in the various solutions showed the same pH influence as for the Na^+ and K^+ concentrations. In the present case, however, the Ca^{2+} concentration decreased with age when $\text{Ca}(\text{OH})_2$ was added to the solution; this behavior was assumed to be due to a traditional pozzolanic reaction, which consists of the combination of the $\text{Ca}(\text{OH})_2$ with the amorphous silica or alumina of the calcined clay to produce hydrated products (ACI Committee 232, 2012).

In addition, when NaOH was incorporated into the solution, the Ca^{2+} concentration decreased even

more. This could be attributed to alkali activation of the sample, as found by Trezza et al. (2020) in Frattini test results of pastes made with portland cement with 25% replacement of calcined illite, and distilled water. The CaO concentration of the contact water decreased when glass powder wastes, which had a high alkali content, were added to the paste to activate the calcined clay.

For the samples in Ca and Ca-Na solution, the influence of treatment temperature was noted in smaller Ca^{2+} concentrations as the temperature increased. In the study of Lemma et al. (2015), in the Frattini test results of the contact water of pastes made with portland cement with 25% replacement of calcined illite, and distilled water, the CaO concentration for each sample decreased with the increment of the treatment temperature. In a more recent study by Lemma et al. (2018), this effect was not evident for temperatures between 900 and 1100°C.

Finally, a relation between $\text{Na}^+ + \text{K}^+$ and Ca^{2+} concentrations (Fig. 9) could be seen, showing a significant Ca^{2+} concentration decrease and a slight $\text{Na}^+ + \text{K}^+$ concentration increase with increasing age and treatment temperature. The influence of the type of solution used on the release of alkalis by samples and, consequently, the influence of solution pH was seen in Fig. 9. In addition, the influence of the treatment temperature was shown by the displacement of the points in the figure to the left and slightly upwards, showing a significant decrease in Ca^{2+} concentration and an increase in the $\text{Na}^+ + \text{K}^+$ concentration with increases in the treatment temperature.

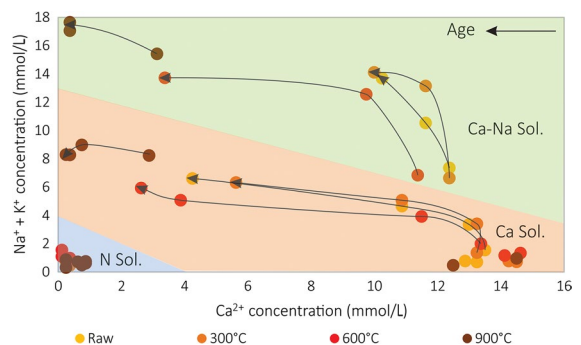


Fig. 9 $\text{Na}^+ + \text{K}^+$ concentration vs. Ca^{2+} concentration of contact water of raw and thermally treated samples in different pH solutions. Age increase follows the arrow, from 7 days to older

Conclusions

When the milled rock, which has a large illite content, is mixed with water or an alkaline solution, a release of Na⁺, K⁺, and Ca²⁺ occurs, which is affected as follows:

- With increasing age, the Na⁺ and K⁺ concentrations increase and the Ca²⁺ concentration decreases.
- Increasing the solution pH increases the Na⁺ and K⁺ concentrations and decreases the Ca²⁺ concentration.
- With increasing treatment temperature, the Na⁺ and K⁺ concentrations increase and the Ca²⁺ concentration decreases until it reaches its activation temperature.

These conclusions are consistent with the proposed hypothesis, so future research will consist of analyzing the alkali release in cementitious systems to evaluate the compressive strength in mortars and ASR tests.

Acknowledgments The authors thank the Facultad de Ingeniería (UNICEN) and the Centro de Geología Aplicada, Agua y Medio Ambiente (CGAMA, CIC-UNS) and the Geology Department of Universidad Nacional del Sur for their support. They also thank Viviana Colasurdo for her help with the alkali-determination techniques.

Funding This work was supported by the Comisión de Investigaciones Científicas de la Provincia de Buenos Aires (CICPBA), the Consejo Nacional de Investigaciones Científicas y Técnicas (CONICET), the Universidad Nacional del Sur, and the Universidad Nacional del Centro de la Provincia de Buenos Aires.

Data Availability Not applicable.

Code Availability Not applicable.

Declarations

Conflicts of Interest/Competing Interests On behalf of all authors, the corresponding author states that there is no conflict of interest.

References

Abedi Koupai, J., Fatahizadeh, M., & Mosaddeghi, M. R. (2020). Effect of pore water pH on mechanical

properties of clay soil. *Bulletin of Engineering Geology and the Environment*, 79(3), 1461–1469. <https://doi.org/10.1007/s10064-019-01611-1>.

ACI Committee 232. (2012). *Report on the Use of Raw or Processed Natural Pozzolans in Concrete*. American Concrete Institute.

Almenares, R. S., Vizcaíno, L. M., Damas, S., Mathieu, A., Alujas, A., & Martirena, F. (2017). Industrial calcination of kaolinitic clays to make reactive pozzolans. *Case Studies in Construction Materials*, 6(January), 225–232. <https://doi.org/10.1016/j.cscm.2017.03.005>.

Ambroise, J., Murat, M., & Péra, J. (1985). Hydration reaction and hardening of calcined clays and related minerals. V. Extension of the research and general conclusions. *Cement and Concrete Research*, 15, 261–268. [https://doi.org/10.1016/0008-8846\(85\)90037-7](https://doi.org/10.1016/0008-8846(85)90037-7).

Andrade, F. A., Al-Qureshi, H. A., & Hotza, D. (2011). Measuring the plasticity of clays: A review. *Applied Clay Science*, 51(1–2), 1–7. <https://doi.org/10.1016/j.clay.2010.10.028>.

Bailey, S.W. (1984). Micas. Illite. In: vol. 13, Reviews in Mineralogy. Mineralogical Society of America, Chantilly, Virginia, USA.

Barrio, C., Poiré, D. G., & Iñiguez, A. M. (1991). El contacto entre la Formación Loma Negra (Grupo Sierras Bayas) y la Formación Cerro Negro, un ejemplo de paleokarst, Olavarría, provincia de Buenos Aires. *Revista de La Asociación Geológica Argentina*, 46(1–2), 69–76.

Batic, O. R., Iñiguez Rodríguez, A. M., & Wainsztein, M. (1971). Puzolanas artificiales obtenidas por tratamiento térmico de arcillas de la provincia de Buenos Aires (1a parte). *Anales LEMIT*, 2(179), 2–20.

Behnood, A., Van Tittelboom, K., & De Belie, N. (2016). Methods for measuring pH in concrete: A review. *Construction and Building Materials*, 105, 176–188. <https://doi.org/10.1016/j.conbuildmat.2015.12.032>.

Benhelal, E., Shamsaei, E., & Rashid, M. I. (2021). Challenges against CO₂ abatement strategies in cement industry: A review. *Journal of Environmental Sciences*, 104, 84–101. <https://doi.org/10.1016/j.jes.2020.11.020>.

Brindley, G. W., & Ali, S. C. (1950). X-ray study of thermal transformations in some magnesian chlorite minerals. *Acta Crystallographica*, 3(1), 25–30. <https://doi.org/10.1107/s0365110x50000069>.

Buchwald, A., Hohmann, M., Posern, K., & Brendler, E. (2009). The suitability of thermally activated illite/smectite clay as raw material for geopolymer binders. *Applied Clay Science*, 46(3), 300–304. <https://doi.org/10.1016/j.clay.2009.08.026>.

Carroll, D., & Starkey, H. C. (1971). Reactivity of clay minerals with acids and alkalis. *Clays and Clay Minerals*, 19(5), 321–333. <https://doi.org/10.1346/CCMN.1971.0190508>.

Cingolani, C. A. (2011). The Tandilia System of Argentina as a southern extension of the Río de la Plata craton: an overview. *International Journal of Earth Sciences*, 100(2–3), 221–242. <https://doi.org/10.1007/s00531-010-0611-5>.

Cordoba, G., & Irassar, E. F. (2021). Sulfate performance of calcined illitic shales. *Construction and Building*

- Materials*, 29(1), 123215. <https://doi.org/10.1016/j.conbuildmat.2021.123215>.
- Cordoba, G., Zito, S. V., Sposito, R., Rahhal, V. F., Tironi, A., Thienel, C., Irassar, E. F., Thienel, K. C., & Irassar, E. F. (2020). Concretes with calcined clay and calcined shale: workability, mechanical, and transport properties. *Journal of Materials in Civil Engineering*, 32(8), 04020224. [https://doi.org/10.1061/\(ASCE\)MT.1943-5533.0003296](https://doi.org/10.1061/(ASCE)MT.1943-5533.0003296).
- Dalla Salda, L., Spalletti, L., Poiré, D., Barrio, R. D. E., & Echeveste, H. (2006). *Tandilia. INSUGEO, Serie Correlación Geológica*, 21(1), 17–46.
- Diop, M. B., & Grutzeck, M. W. (2008). Sodium silicate activated clay brick. *Bulletin of Engineering Geology and the Environment*, 67(4), 499–505. <https://doi.org/10.1007/s10064-008-0160-3>.
- Fernandez, R., Martirena, F., & Scrivener, K. L. (2011). The origin of the pozzolanic activity of calcined clay minerals: A comparison between kaolinite, illite and montmorillonite. *Cement and Concrete Research*, 41(1), 113–122. <https://doi.org/10.1016/j.cemconres.2010.09.013>.
- Folliard, K. J., Thomas, M. D. A., & Kurtis, K. E. (2003). FHWA-RD-03-047 Guidelines for the use of lithium to mitigate or prevent Alkali-Silica Reaction (ASR). *FHWA-RD-03-047*. <https://www.fhwa.dot.gov/publications/research/infrastructure/pavements/pccp/03047/index.cfm>.
- Grim, R. E. (1942). Modern concepts of clay materials. *Journal of Geology*, L(3), 225–275.
- Hanein, T., Thienel, K. C., Zunino, F., Marsh, A. T. M., Maier, M., Wang, B., Canut, M., Juenger, M. C. G., Ben Haha, M., Avet, F., Parashar, A., Al-Jaberi, L. A., Almenares-Reyes, R. S., Alujas-Diaz, A., Scrivener, K. L., Bernal, S. A., Provis, J. L., Sui, T., Bishnoi, S., & Martirena-Hernández, F. (2022). Clay calcination technology: state-of-the-art review by the RILEM TC 282-CCL. *Materials and Structures/Materiaux et Constructions*, 55(1). <https://doi.org/10.1617/s11527-021-01807-6>.
- He, C., Makovicky, E., & Øsbaeck, B. (1995a). Thermal stability and pozzolanic activity of calcined illite. *Applied Clay Science*, 9(5), 337–354. [https://doi.org/10.1016/0169-1317\(94\)00033-M](https://doi.org/10.1016/0169-1317(94)00033-M).
- He, C., Osbaeck, B., & Makovicky, E. (1995b). Pozzolanic reactions of six principal clay minerals: Activation, reactivity assessments and technological effects. *Cement and Concrete Research*, 25(8), 1691–1702. [https://doi.org/10.1016/0008-8846\(95\)00165-4](https://doi.org/10.1016/0008-8846(95)00165-4).
- Hu, N., Bernsmeier, D., Grathoff, G. H., & Warr, L. N. (2017). The influence of alkali activator type, curing temperature and gibbsite on the geopolymerization of an interstratified illite-smectite rich clay from Friedland. *Applied Clay Science*, 135, 386–393. <https://doi.org/10.1016/j.clay.2016.10.021>.
- Irassar, E. F., Bonavetti, V. L., Castellano, C. C., Trezza, M. A., Rahhal, V. F., Cordoba, G., & Lemma, R. (2019). Calcined illite-chlorite shale as supplementary cementing material: Thermal treatment, grinding, color and pozzolanic activity. *Applied Clay Science*, 179(January), 105143. <https://doi.org/10.1016/j.clay.2019.105143>.
- Jiang, T., Li, G., Qiu, G., Fan, X., & Huang, Z. (2008). Thermal activation and alkali dissolution of silicon from illite. *Applied Clay Science*, 40(1–4), 81–89. <https://doi.org/10.1016/j.clay.2007.08.002>.
- Lemma, R., Irassar, E. F., & Rahhal, V. F. (2015). Calcined illitic clays as portland cement replacements. *Calcined Clays for Sustainable Concrete, RILEM Bookseries*, 10. <https://doi.org/10.1007/978-94-017-9939-3>.
- Lemma, R., Castellano, C. C., Bonavetti, V. L., Trezza, M. A., Rahhal, V. F., & Irassar, E. F. (2018). Thermal transformation of illitic-chlorite clay and its pozzolanic activity. *Calcined Clays for Sustainable Concrete, RILEM Bookseries*, 16, 266–272. https://doi.org/10.1007/978-94-024-1207-9_43.
- Marchetti, G., Rahhal, V., Pavlík, Z., Pavlíková, M., & Irassar, E. F. (2020). Assessment of packing, flowability, hydration kinetics, and strength of blended cements with illitic calcined shale. *Construction and Building Materials*, 254, 119042. <https://doi.org/10.1016/j.conbuildmat.2020.119042>.
- Marsh, A., Heath, A., Patureau, P., Evernden, M., & Walker, P. (2018). Alkali activation behaviour of un-calcined montmorillonite and illite clay minerals. *Applied Clay Science*, 166(February), 250–261. <https://doi.org/10.1016/j.clay.2018.09.011>.
- Mikulčić, H., Klemeš, J. J., Vujanović, M., Urbanec, K., & Duić, N. (2016). Reducing greenhouse gases emissions by fostering the deployment of alternative raw materials and energy sources in the cleaner cement manufacturing process. *Journal of Cleaner Production*, 136, 119–132. <https://doi.org/10.1016/j.jclepro.2016.04.145>.
- Murad, E., & Wagner, U. (1996). The thermal behaviour of an Fe-rich illite. *Clay Minerals*, 31(1), 45–52. <https://doi.org/10.1180/claymin.1996.031.1.04>.
- Nickovic, S., Vukovic, A., Vujadinovic, M., Djurdjevic, V., & Pejanovic, G. (2012). Technical Note: High-resolution mineralogical database of dust-productive soils for atmospheric dust modeling. *Atmospheric Chemistry and Physics*, 12(2), 845–855. <https://doi.org/10.5194/acp-12-845-2012>.
- Pérez Marfil, P., Locati, F., Marfil, S., & Falcone, D. (2021). Assessment of the potential alkali-reactivity of slow-reacting aggregates from the province of Buenos Aires, Argentina. *Bulletin of Engineering Geology and the Environment*, 80(12), 8935–8948. <https://doi.org/10.1007/s10064-019-01551-w>.
- Rossetti, A., Cordoba, G. P., Falcone, D., & Irassar, E. F. (2018). Estudios de arcillas calcinadas illíticas como posibles inhibidoras de la reacción álcali sílice. *VIII Congreso Internacional - 22a Reunión Técnica de La AATH*, 163–170.
- Sabir, B., Wild, S., & Bai, J. (2001). Metakaolin and calcined clays as pozzolans for concrete: a review. *Cement and Concrete Composites*, 23(6), 441–454. [https://doi.org/10.1016/S0958-9465\(00\)00092-5](https://doi.org/10.1016/S0958-9465(00)00092-5).
- Scrivener, K. L., John, V. M., & Gartner, E. M. (2018). Eco-efficient cements: Potential economically viable solutions for a low-CO₂ cement-based materials industry. *Cement and Concrete Research*, 114(February), 2–26. <https://doi.org/10.1016/j.cemconres.2018.03.015>.
- Sruthi, P. L., & Reddy, P. H. P. (2020). Effect of alkali concentration on swelling characteristics of transformed kaolinitic clays. *Clays and Clay Minerals*, 68, 373–393. <https://doi.org/10.1007/s42860-020-00081-x>.

- Tam, C., Taylor, M., Gielen, D., Twigg, C., Klee, H., Rocha, P., & Meer, R. van der. (2009). *Cement technology roadmap 2009 - Carbon emissions reductions up to 2050*.
- Trezza, M. A., Irassar, E. F., & Rahhal, V. F. (2020). Alkaline activation of blended cements with calcined illitic clay using glass powder wastes. *RILEM Bookseries*, 25, 115–124. https://doi.org/10.1007/978-981-15-2806-4_13.
- Trümer, A., & Ludwig, H. M. (2015). Sulphate and ASR resistance of concrete made with calcined clay blended cements. *RILEM Bookseries*, 10, 3–9. https://doi.org/10.1007/978-94-017-9939-3_1.
- Werling, N., Kaltenbach, J., Weidler, P. G., Schuhmann, R., Dehn, F., & Emmerich, K. (2022). Solubility of calcined kaolinite, montmorillonite, and illite in high molar NaOH and suitability as precursors for geopolymers. *Clays and Clay Minerals*, 70(2), 270–289. <https://doi.org/10.1007/s42860-022-00185-6>.
- Zalba, P. E., Morosi, M., Conconi, M. S., & Segovia, L. (2010). Arcillas de Tandilia. Geología, mineralogía y propiedades tecnológicas. *CIC. Editorial Universitaria de La Plata*.

Springer Nature or its licensor (e.g. a society or other partner) holds exclusive rights to this article under a publishing agreement with the author(s) or other rightsholder(s); author self-archiving of the accepted manuscript version of this article is solely governed by the terms of such publishing agreement and applicable law.